Graphical representation of the temporal patterns of trait evolution in Lake Tanganyika cichlids based on alternative time-calibrated species trees (Fig. D1-D3), based on samples from the posterior tree distribution for each alternative species tree (Fig. D4-D6), and based on PC1-scores of the morphological traits (Fig. D7). Inferred rates of trait evolution per tribe are shown in Fig. D8.

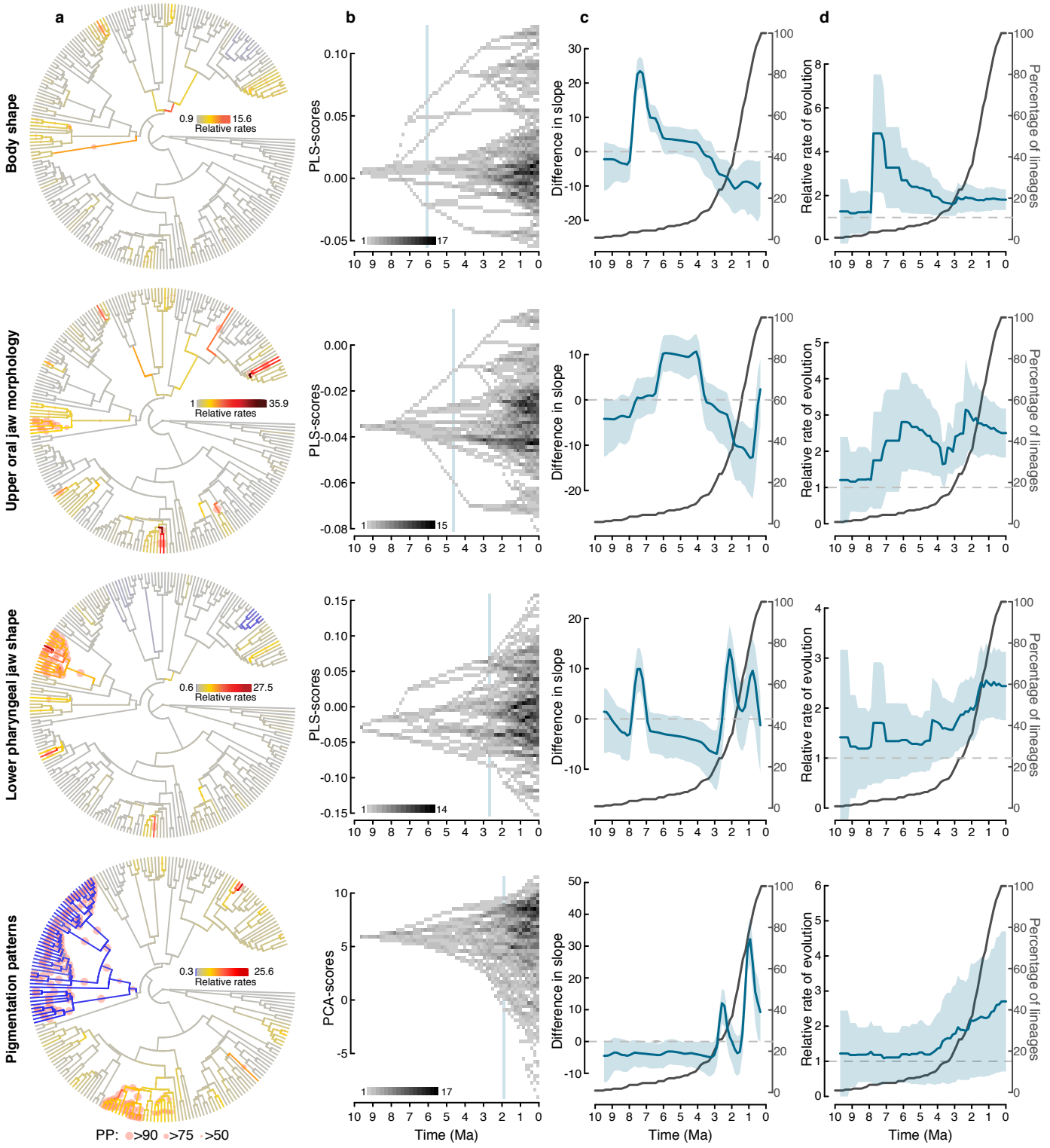

Fig. D1 I Temporal dynamics of diversification in body shape (first row), upper oral jaw morphology (second row), lower pharyngeal jaw shape (third row), and pigmentation patterns (fourth row). a, Time-calibrated species tree (maximum likelihood tree topology inferred from genome-wide SNPs, as shown in Fig. 1 of the manuscript), with branches coloured according to the mean relative rates of trait evolution for each trait. **b**, Morphospace densities (number of lineages) through time for each trait. **c**, Comparison of slopes (blue) of morphospace expansion over time between the observed data and the BM null model of trait evolution. The shaded areas show 95% quantiles of the 500 BM simulations. Lineage accumulation through time derived from the species tree is shown in dark grey. **d**, Mean relative rates of trait evolution over time with standard deviation (blue). Lineage accumulation through time is shown in dark grey.

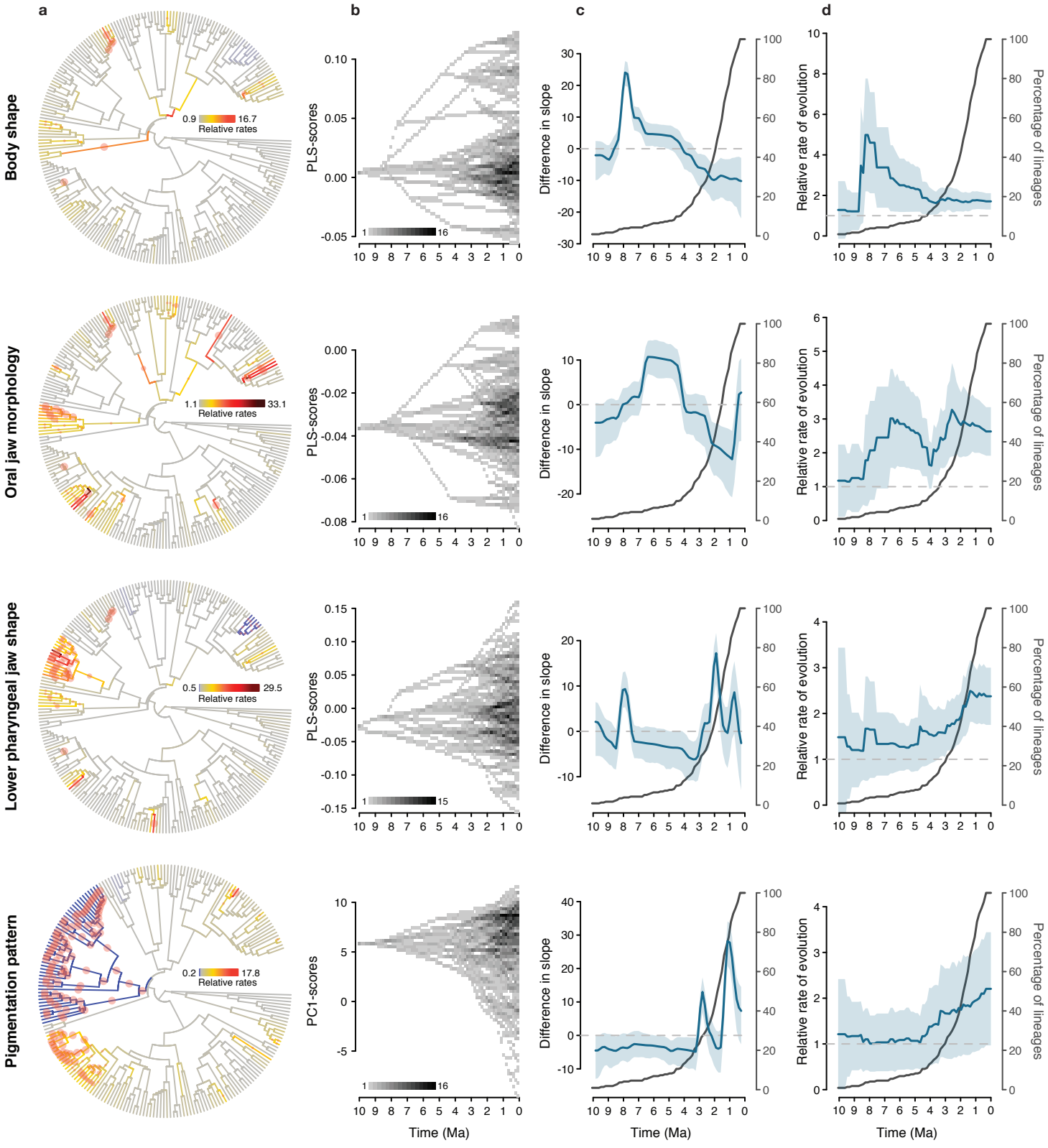

Fig. D2 | Temporal dynamics of diversification in body shape (first row), upper oral jaw morphology (second row), lower pharyngeal jaw shape (third row), and pigmentation patterns (fourth row) based on an alternative time-calibrated species tree. a, Species tree based on the tree topology inferred with ASTRAL from selected genomic regions under the multi-species coalescent model, time-calibrated using the relaxed molecular-clock model. Branches are coloured according to the mean relative rates of trait evolution for each trait. **b**, Morphospace densities (number of lineages) through time for each trait. **c**, Comparison of slopes (blue) of morphospace expansion over time between the observed data and the BM null model of trait evolution. The shaded areas show 95% quantiles of the 500 BM simulations. Lineage accumulation through time derived from the species tree is shown in dark grey. **d**, Mean relative rates of trait evolution over time with standard deviation (blue). Lineage accumulation through time is shown in dark grey.

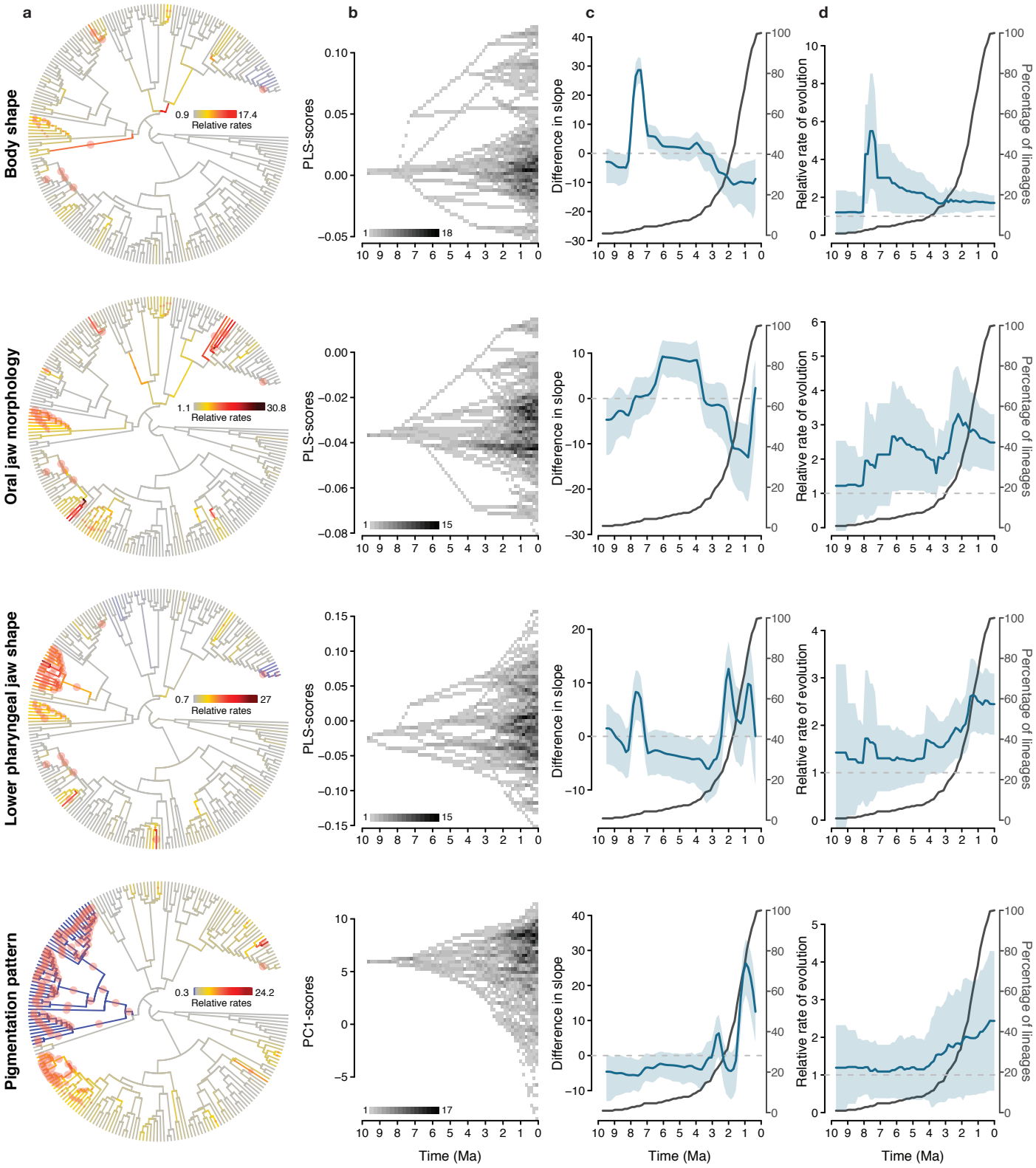

Fig. D3 I Temporal dynamics of diversification in body shape (first row), upper oral jaw morphology (second row), lower pharyngeal jaw shape (third row), and pigmentation patterns (fourth row) based on an alternative time-calibrated species tree. a, Species tree based on the tree topology inferred with SNAPP from genome wide SNP data under the multi-species coalescent model, time-calibrated using the relaxed molecular-clock model. Branches are coloured according to the mean relative rates of trait evolution for each trait. **b**, Morphospace densities (number of lineages) through time for each trait. **c**, Comparison of slopes (blue) of morphospace expansion over time between the observed data and the BM null model of trait evolution. The shaded areas show 95% quantiles of the 500 BM simulations. Lineage accumulation through time derived from the species tree is shown in dark grey. **d**, Mean relative rates of trait evolution over time with standard deviation (blue). Lineage accumulation through time is shown in dark grey.

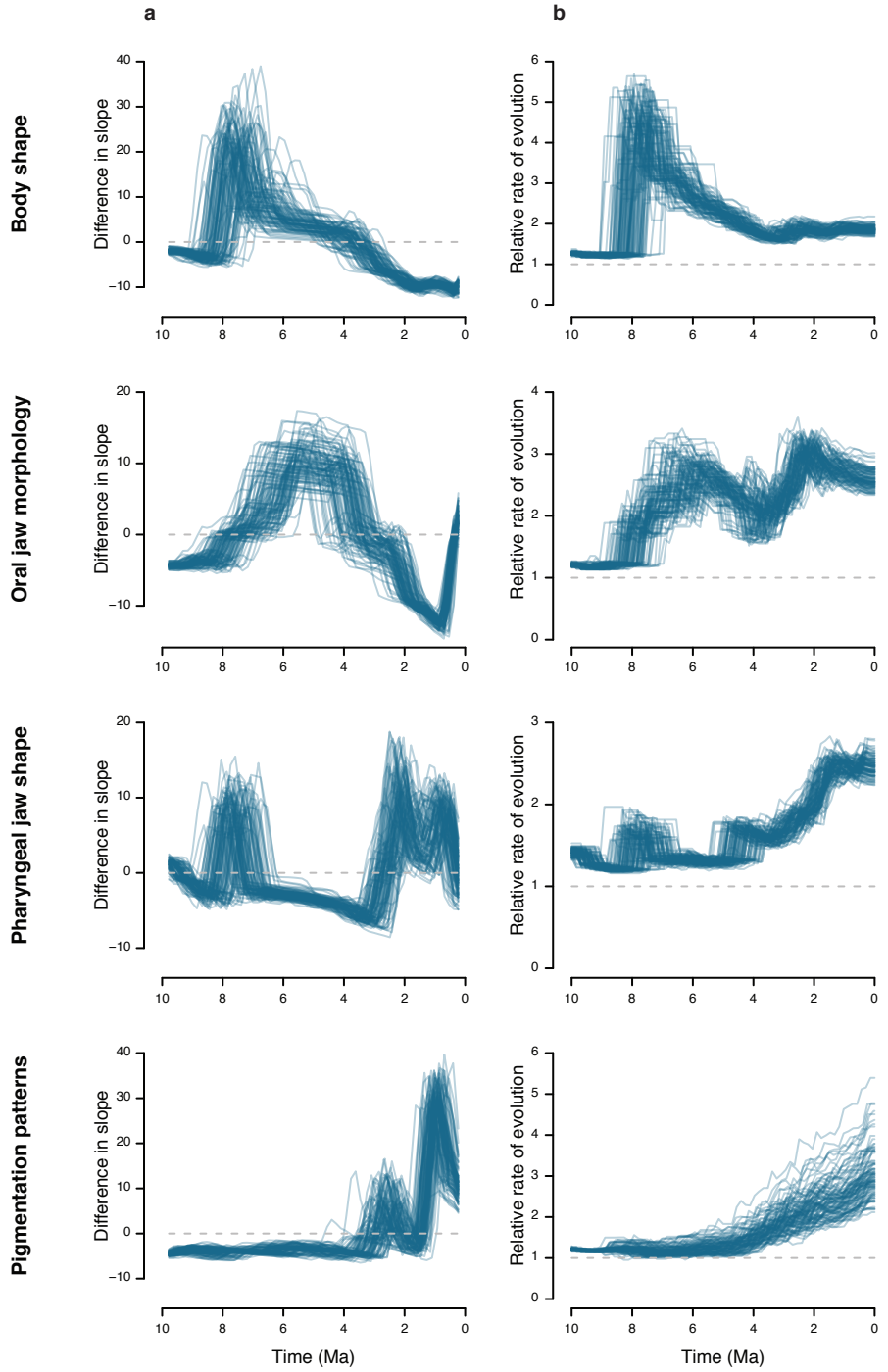

Fig. D4 | Temporal dynamics of diversification in body shape (first row), upper oral jaw morphology (second row), lower pharyngeal jaw shape (third row), and pigmentation patterns (fourth row) based on the posterior distribution of the time-calibration. Results from 100 trees sampled from the posterior distribution of the time-calibration for the maximum likelihood tree topology inferred from genome-wide SNPs. Each line represents the mean of the results based on a one posterior tree, plotted on a relative timescale of 10-0 Ma for better visualization (true root ages of the 100 trees range from 8.79-10.41 Myr) **a**, Comparison of slopes of morphospace expansion over time between the observed data and the BM null model of trait evolution. **b**, Mean relative rates of trait evolution over time.

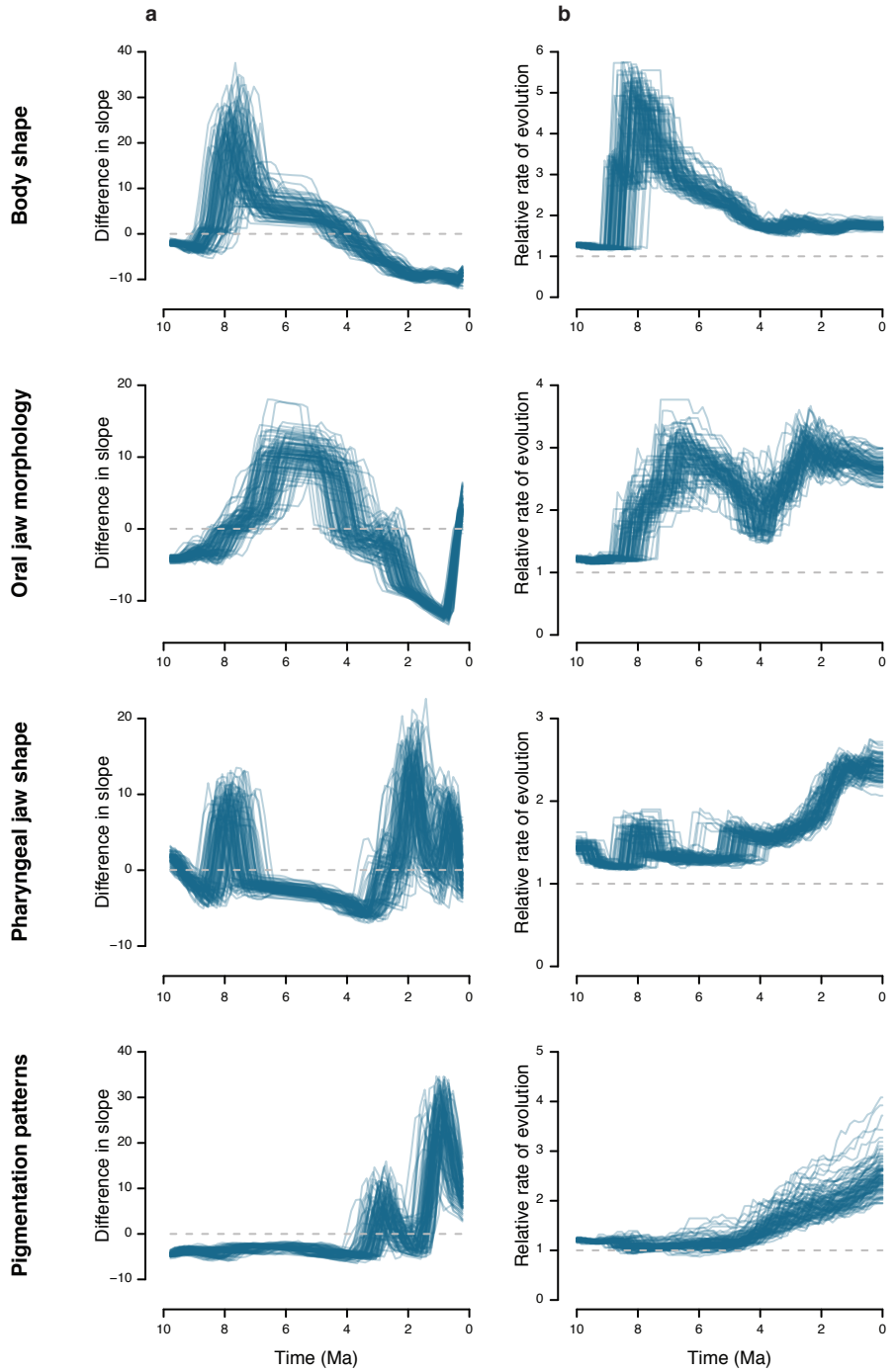

Fig. D5 | Temporal dynamics of diversification in body shape (first row), upper oral jaw morphology (second row), lower pharyngeal jaw shape (third row), and pigmentation patterns (fourth row) based on the posterior distribution of the time-calibration. Results from 100 trees sampled from the posterior distribution of the time-calibration for the tree topology based on selected genomic regions inferred under the multi-species coalescent model with ASTRAL. Each line represents the mean of the results based on a one posterior tree, plotted on a relative timescale of 10-0 Ma for better visualization (true root ages of the 100 trees range from 9.41-10.86 Myr) **a**, Comparison of slopes of morphospace expansion over time between the observed data and the BM null model of trait evolution. **b**, Mean relative rates of trait evolution over time.

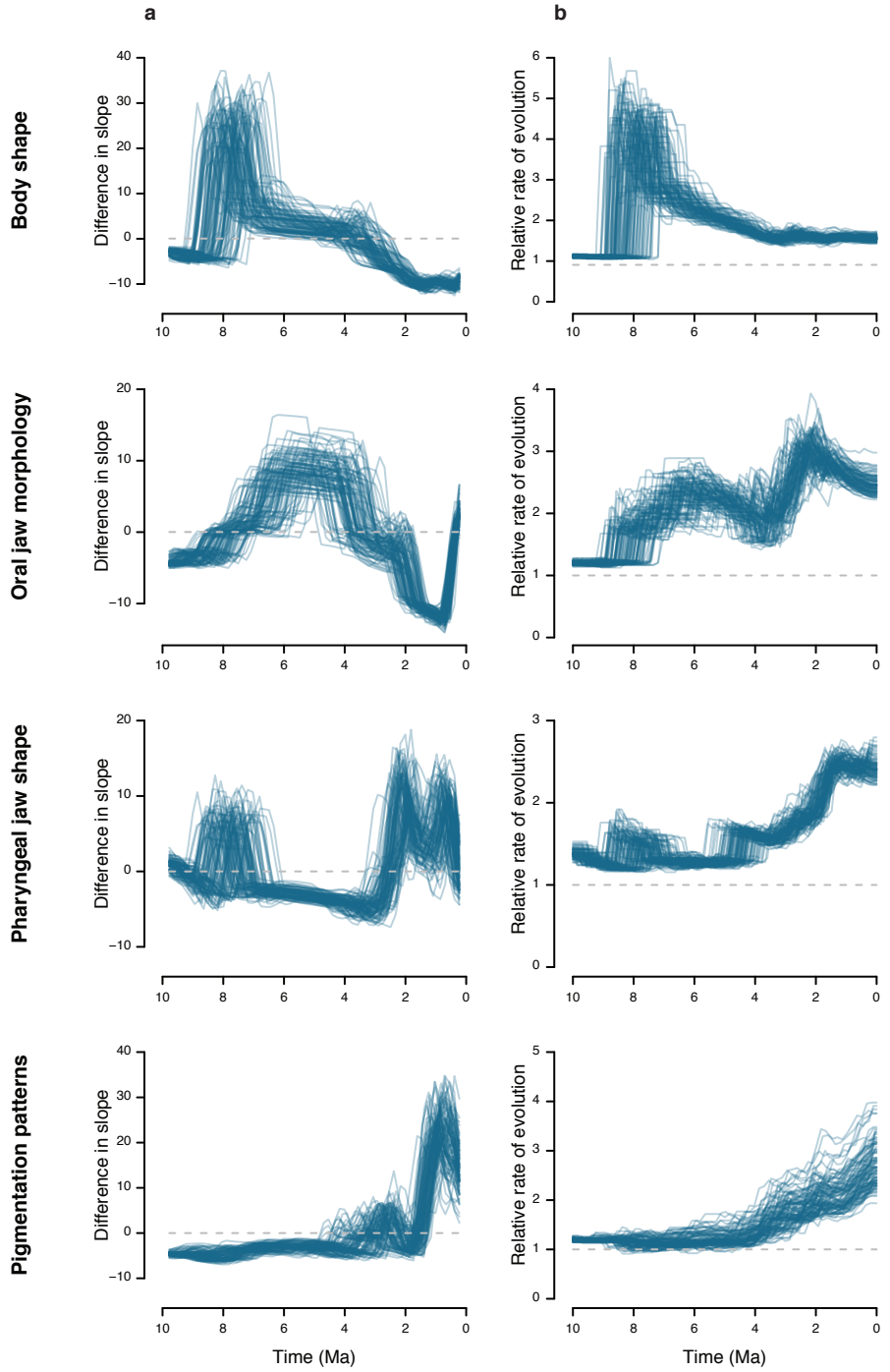

Fig. D6 | Temporal dynamics of diversification in body shape (first row), upper oral jaw morphology (second row), lower pharyngeal jaw shape (third row), and pigmentation patterns (fourth row) based on the posterior distribution of the time-calibration. Results from 100 trees sampled from the posterior distribution of the time-calibration for the tree topology based on genome-wide SNPs inferred under the multi-species coalescent model with SNAPP. Each line represents the mean of the results based on a one posterior tree, plotted on a relative timescale of 10-0 Ma for better visualization (true root ages of the 100 trees range from 9.05-10.46 Myr) **a**, Comparison of slopes of morphospace expansion over time between the observed data and the BM null model of trait evolution. **b**, Mean relative rates of trait evolution over time.

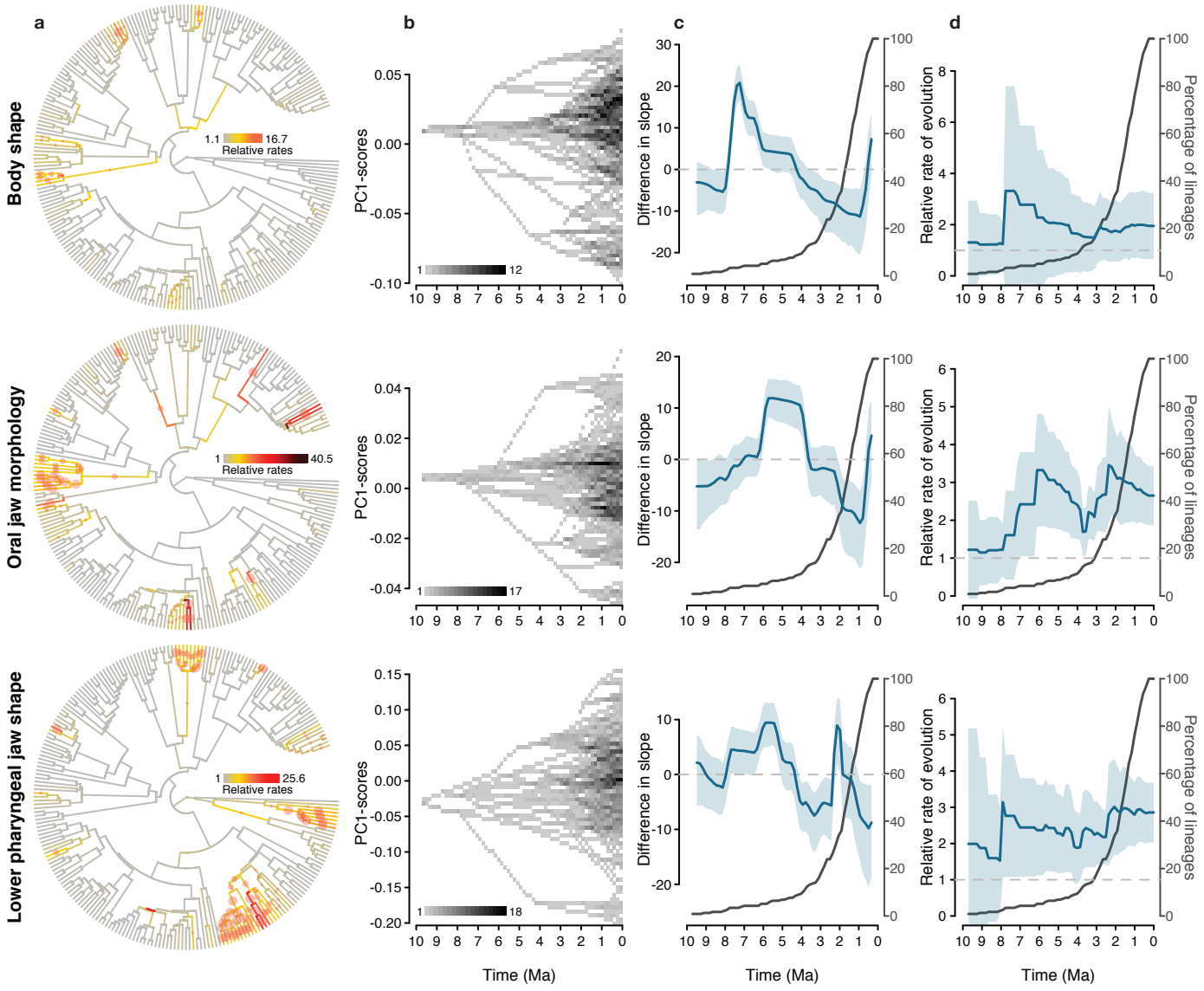

Fig. D7 I Temporal dynamics of diversification in body shape (first row), upper oral jaw morphology (second row), and lower pharyngeal jaw shape (third row) using PC1-scores. a, Time-calibrated species tree (maximum likelihood tree topology inferred from genome-wide SNPs, as shown in Fig. 1 of the manuscript), with branches coloured according to the mean relative rates of trait evolution for each trait. **b**, Morphospace densities (number of lineages) through time for each trait. **c**, Comparison of slopes (blue) of morphospace expansion over time between the observed data and the BM null model of trait evolution. The shaded areas show 95% quantiles of the 500 BM simulations. Lineage accumulation through time derived from the species tree is shown in dark grey. **d**, Mean relative rates of trait evolution over time with standard deviation (blue). Lineage accumulation through time is shown in dark grey.

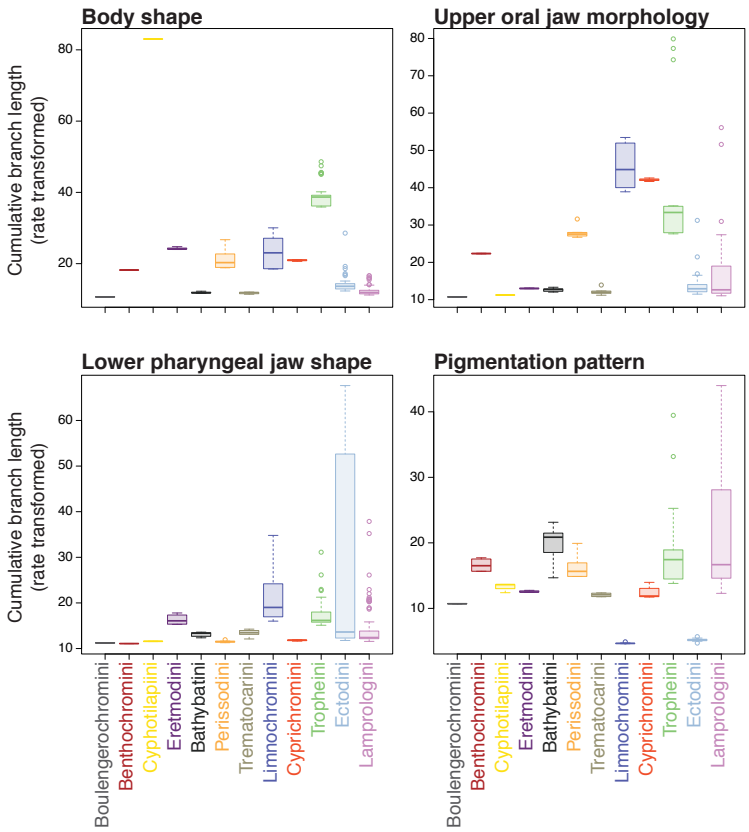

Fig. D8 | Cumulative rate-transformed branch length per tribe and trait. Boxplot per tribe of the cumulative rate-transformed branch length derived from the variable rates model using the time-calibrated species tree (maximum likelihood tree topology). Thus, species values represent time-weighted estimates over the inferred evolutionary rates.